2013 International Conference on Indoor Positioning and Indoor Navigation, 28-31st October 2013

Ultrasonic LPS Adaptation for Smartphones

David Gualda, Mª Carmen Pérez, Jesús Ureña, Juan C. García, Daniel Ruiz, Enrique García, Alejandro Lindo
Electronics Department, Alcala de Henares University
Alcalá de Henares, Madrid, Spain
E-mail: {david.gualda, carmen}@depeca.uah.es

Abstract— **In this paper we present a privacy-oriented Ultrasonic Local Positioning System (U-LPS) allowing users with portable devices, such as smartphones or tablets, to accurately determine their position in indoor environments. Indoor U-LPSs have been widely used to provide location information with centimeter or even sub-centimeter level accuracy at high rates. However, most of these systems demand specific hardware in the reception stage that cannot be used with current smartphones. Hence, the user cannot benefit from the versatility of services that these kind of devices offer. This work presents the design of an external device which translates the high frequency ultrasonic information emitted by a CDMA-based U-LPS, into a low frequency band understandable for the mobile phone by means of an analog multiplier. The output of the multiplier is connected to the smartphone or tablet using the Jack input connector as if it was a microphone. Then, the mobile device processes the low band frequency signals and estimates its position.**

Keywords-component; LPS, Analog Multiplier, Kasami, Smartphone.

I. INTRODUCTION

Whereas outdoor positioning systems for smartphones or tablets are highly developed, indoor positioning for this kind of mobile devices is not operating at the same level. Radio-Frequency (RF) signals are the most used for locating commercial smartphones in indoor environments; however they report poor accuracy (meter-level) [1]-[3]. In contrast, Ultrasonic Local Positioning Systems (U-LPSs) are one of the best options to implement indoor localization systems when centimeter or even millimeter-level accuracy is required [4]-[6]. Furthermore ultrasonic localization systems have some advantages over RF based systems like the lower speed of propagation of ultrasonic signals or its simplicity to model and control for indoor environments since they do not propagate through walls [7].

Despite of its great accuracy, most U-LPS are not available for smartphones or tablets, so they cannot offer the variety of services of these devices, which include web-applications and multimedia services for user interaction or augmented reality. Smartphones and tablets do not work properly with ultrasonic signals higher than 22 kHz frequency, while U-LPSs use to work at frequencies of about 40 kHz. To overcome this problem, a very recent work [8] proposes a centralized U-LPS, where the mobile phone transmits at 20-22 kHz range. The emitted signal is received by a set of four ultrasound microphones placed at known positions in the environment, which synchronously send the data gathered to a centrally-controlled service (a personal computer) that computes the time-differences of arrival (TDOA), obtaining average accuracies about 10 cm. Instead, we propose a privacy oriented system, preventing the user from being in control by a central service, what can cause some concern about how location information is being handled [9]. Also, an important contribution of our proposal is to permit the coexistence of an unlimited number of users computing their location through their mobile phones or tablets. It can be useful, for instance, in a context-aware commercial area or museum where all visitors can simultaneously enhance their experience.

The proposal of this work is the development of an indoor positioning system for smartphones or tablets adapting the emitted signals coming from an U-LPS. The U-LPS consists of a set of five beacons placed at known positions of the environment, all of them transmitting in a simultaneous and periodic way. To achieve the simultaneous emission, Code Division Multiple Access (CDMA) techniques have been used. Thus, each beacon transmits a different 1023 Kasami code, which has been BPSK modulated with a 40 kHz carrier. These codes have been chosen due to its good auto-correlation and cross-correlation properties. In the reception stage, we have designed an external device to be connected with the smartphone. It translates the high frequency ultrasonic information coming from an ultrasonic receiver into a low frequency band by means of an analog multiplier. The output of the multiplier is connected to the smartphone or tablet using the Jack input connector as if it was a microphone. Finally, the mobile device processes the low band frequency signals and estimates the position by means of a hyperbolic trilateration algorithm based on the Gauss Newton minimization method [10]. Hyperbolic trilateration avoids the use of additional hardware, such as RF or infrared signals, to synchronize emitters and receivers. The error in the position estimation using the proposed method is similar to the obtained with the original U-LPS using an ultrasonic receiver with its ad-hoc processing hardware.

978-1-4799-4043-1/13/$31.00 ©2013 IEEE

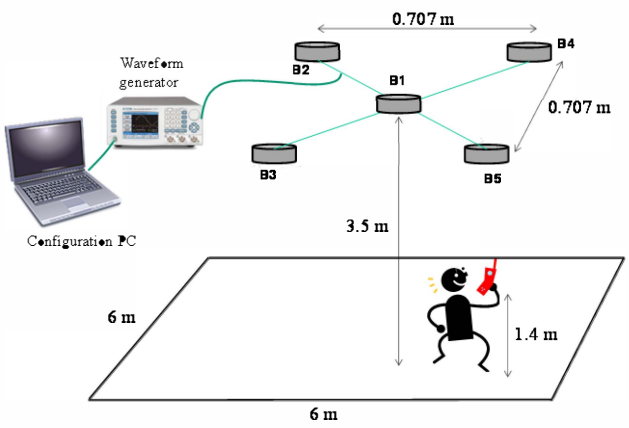

Fig. 1.- Schematic representation of the U-LPS.

The rest of the paper is organized as follows: Section II explains the U-LPS and the common detection process for traditional U-LPS and the one proposed here for smartphones or tablets. In Section III the reception stage is adapted taking into account the smartphone/tablet requirements. In Section IV some results obtained with the proposed system are provided and compared with those obtained with standard ad-hoc processing hardware. Finally, conclusions are discussed in Section V.

II. ULTRASONIC LOCAL POSITIONING SYSTEM

A. *Arquitecture of the U-LPS*

Fig. 1 is a general view of the proposed U-LPS. A set of five beacons, oriented downwards, are placed at known positions of the environment, covering an area of 36 m^2. At the reception, a non-limited number of portable receivers (smartphones, tablets or similar) can compute autonomous and independently their position by hyperbolic trilateration. The proposed system can be extended to provide a high cover area by using several U-LPS as indicated in [11].

B. *Beacon system*

The ultrasonic beacon system has been placed in the ceiling of the environment to be covered, at a height of 3.50 m. It consists of five transducers, located into a 0.707 m x 0.707 m surface, as Fig. 2 shows. The beacons are wired-synchronized, allowing simultaneous and periodic emission.

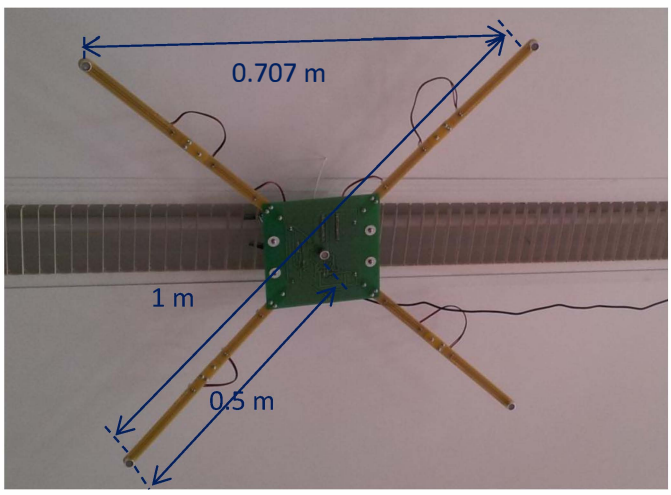

Fig. 2.- View of the U-LPS.

To avoid Mutual Access Interferences (MAI) among beacons, all of them are encoded with a different 1023-bit Kasami code [12]. These codes have been selected due to their suitable auto-correlation and cross-correlation results, even after the modulation process (see Fig. 3 for an example of correlation results for BPSK-modulated 1023-Kasami codes). The modulation allows the spectrum of the emitted signal to be centered at the central frequency of the transducer.

Specifically, the ultrasonic transducer used as beacon is the Prowave 328ST160 [13]. This transducer has an aperture angle of ±80º, and by testing it in an isolated chamber, the frequency response of Fig. 4 has been obtained. It shows a first resonance peak at 32.8 kHz, with a bandwidth of 2.5 kHz; but also, a second resonance peak at 46 kHz. Therefore, to obtain a 18 kHz bandwidth, the transducers have been excited by the Kasami code modulated with a carrier of central frequency f_c=40 kHz.

All transducers are connected to a waveform generator [14] which is controlled by a Personal Computer (PC). In the PC the type of binary sequence used and its length can be configured. On the other hand, the type of carrier used in the modulation (sinusoidal or square), the number of carrier periods and the time interval between emissions can be also

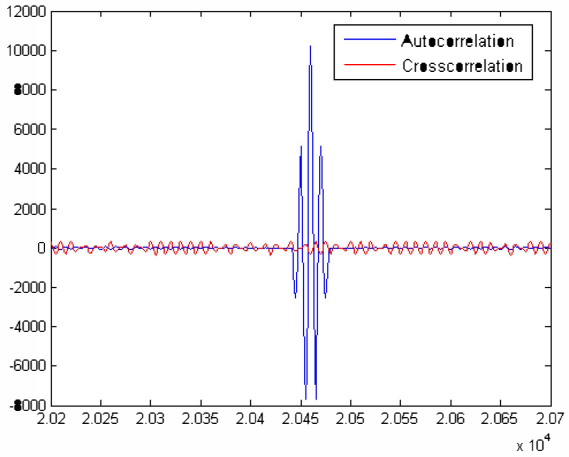

Fig. 3.- Auto-correlation (blue) and cross-correlation (red) of a Kasami code of 1023 bits BPSK modulated with a carrier frequency of 40 kHz.

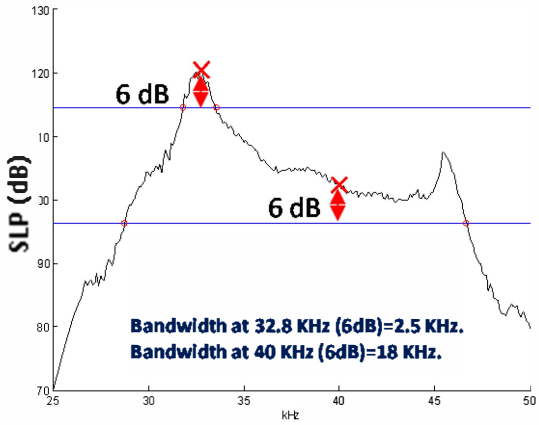

Fig. 4.- Prowave 328T160 frequency response.

selected. The codes are generated and BPSK modulated off-line. A digital pass-band filter with 40 kHz central frequency and 10 kHz bandwidth has been included to only consider the information within the ultrasonic transducer bandwidth. The obtained signals are sent to the waveform generator, which transmit them in a synchronous way.

C. *Reception stage*

In the reception stage, each mobile device computes its position by hyperbolic trilateration of the distances obtained from the measurement of the time-differences of arrival (TDOA) between a reference beacon (the nearest one) and the others [10]. To detect the TDOAs, each mobile device performs the simultaneous generalized cross-correlation (GCC) of the received signal, after being demodulated, with the codes assigned to each beacon. A peak indicating the arrival instant of each code will be obtained at the output of the corresponding GCC block (in absolute value). Then, the time delay corresponding to the reference beacon is subtracted to obtain the TDOAs. A GCC algorithm [15] has been chosen instead of traditional correlation since it provides a significant reduction on the lateral lobe effects, what makes easier the detection of the maximum peak that determines the arrival instant of each sequence. Fig. 5 is a comparison of the correlation peaks obtained after the GCC and the standard correlation when the signal emitted from beacon 2 is detected, considering a signal-to-noise ratio (SNR) of 10 dB and the five beacons emitting simultaneously. Clearly the peak showing the arrival of the sequence Kasami for beacon 2 can be better detected in case of the GCC. For further details regarding the GCC and its performance in an U-LPS see [16].

Fig. 6 summarizes the processing carried out in each mobile device when traditional U-LPS are used (hereon U-LPS$_T$). The acquisition system adapts the signal received by the ultrasonic microphone to the input range of an analog-to digital (A/D) converter. Then, low-level and high-level tasks can be carried out in a PC. Some works [6][17] use FPGA-based implementations instead for the real-time processing of the correlation stage. For better understanding, we have called U-LPS$_N$ the new proposal for smartphones or tablets. In that case, the low-level and high-level tasks are performed within

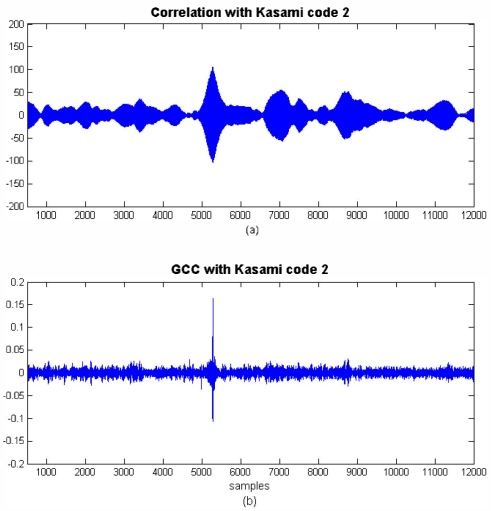

Fig. 5.- Time arrival detection of the sequence corresponding to beacon 2: (a) by using standard correlation, (b) by using GCC.

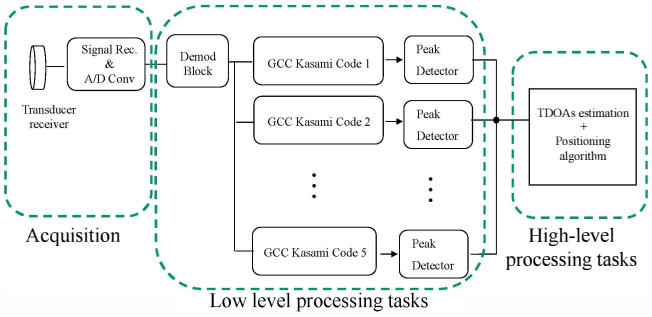

Fig. 6.- Block diagram of the processing at the receiver in a U-LPS$_T$.

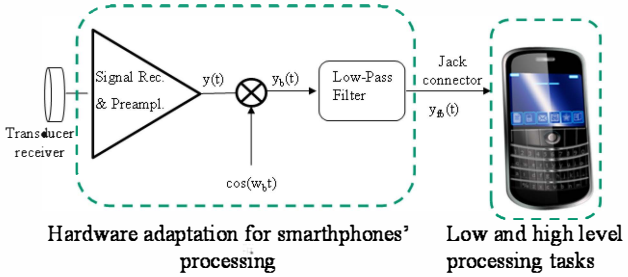

Fig. 7.- Hardware adaptation for processing the ultrasonic signals coming from the beacons with the smartphone in the U-LPS$_N$.

the mobile device. The acquisition system and low-level processing have to be modified as indicated in Section III.

III. RECEIVER ADAPTATION FOR SMARTPHONES POSITIONING

Fig. 7 shows the proposed hardware to adapt the ultrasonic signals coming from the beacons to the smartphone or tablet processing capabilities. The received signal $y(t)$, after the conditioning and amplification stage, is analogically multiplied by a cosine with frequency f_b kHz in order to translate the high frequency information emitted by the beacons into the low frequency band that can manage the mobile phone. Eq. (1) summarizes the process:

$$y_b(t) = y(t) \cdot \cos(2\pi f_b t)$$
$$y(t) = \sum_{j=1}^{J} x_j * h_j(t, \tau_j) + \eta(t) \quad (1)$$

Where $y(t)$ is the received and amplified signal and $y_b(t)$ is the signal after the frequency down translation. The encoded emission for beacon j is x_j, $0 \leq j \leq J$, where J is the number of beacons considered. Note that x_j is the result of the BPSK modulation of a Kasami code c_j of length L with N_{SM} periods of a sinusoidal carrier $s(t)$ with frequency $f_c = 1/T_c$ -see Eq. 2-. As well as this, $h_j(t,\tau_j)$ is the response of the channel for beacon j (including emitter and receiver); τ_j is the delay in receiving the sequence assigned to beacon j and $\eta(t)$ is a zero-

mean Gaussian noise with variance σ^2. Finally, * is the convolution operation.

$$x_j(t) = \sum_{i=0}^{L-1} c_j[i] \cdot s(t - i \cdot N_{SM} \cdot T_c); \qquad (2)$$

$$s(t) \quad \rightarrow N_{SM} \ periods \ of \cos(2\pi f_c t)$$

The spectrum of $x_j(t)$, $X_j(\omega)$ is roughly centered around f_c, as well as the spectrum of $y(t)$, $Y(\omega)$, in this case with a bandwidth which depends on N_{SM} and $h_j(t,\tau_j)$. As this signal is bandlimitted the down traslation in frequency is performed using the modulation theorem:

$$\begin{aligned} y(t) \quad &\leftrightarrow \quad Y(\omega) \\ y_b(t) = y(t) \cdot \cos(2\pi f_b t) \quad &\leftrightarrow \quad Y_b(\omega) = \frac{1}{2}\left[Y(\omega - 2\pi f_b) + Y(\omega + 2\pi f_b)\right] \end{aligned} \qquad (3)$$

Considering that $f_c=40$ kHz, $f_b=30$ kHz, $N_{SM}=2$ and $J=5$, the signal after the frequency down translation will concentrate its energy around 10 kHz and 70 kHz. Then, a low-pass filter with cutoff frequency of 20 kHz has been included to only consider the frequency range of interest in the smartphone. The output of the low-pass filter $y_{fb}(t)$ is connected to the smartphone or tablet by using the Jack input connector.

Fig. 8a shows the estimated spectrum of one of the emitted codes x_j after the modulation process. Fig. 8b shows the estimated spectrum of the received signal $y(t)$ when a SNR= 10 dB is considered. As well as this, Fig. 8c depicts the estimated spectrum after the analog multiplier, that is, $y_b(t)$; and finally, Fig. 8d is the estimated spectrum after the low-pass filtering.

Once in the mobile device, the high level processing program is the same that was indicated in Section II.C. On the other hand, the low-level processing algorithm changes in this case. The reference signal for each GCC to be performed in order to search for possible emissions coming from the beacons, is the Kasami code generated in high frequency (40 kHz) and digitally down translate in frequency (performing the multiplication by the 30 kHz cosine) and after low-pass filtered. With that purpose, we have simulated in Matlab® the processing described in Fig. 7 independently for each modulated Kasami code, that is, in each simulation $y_j(t)=x_j(t)$. Then, the output $y_{fb_j}(t)$ is stored and used by the mobile phone as pattern for the GCC with the input signal, even when real signals are involved. If the model of the beacon transducer is available, its effect can also be included in the code-pattern to be stored for the GCC.

IV. RESULTS

A. SIMULATED RESULTS

The proposed U-LPS$_N$ has been initially simulated, not only to validate its feasibility but also to compare the results

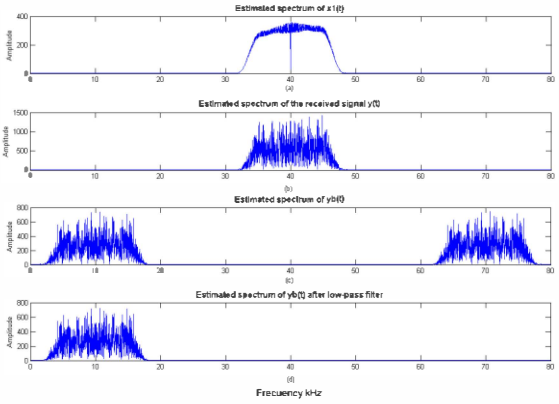

Fig. 8.- Estimated spectrum at each stage of the proposed hardware adaptation of Fig. 7.

obtained with those of a traditional U-LPS$_T$ based on specialized hardware not available on current phones. With that purpose, the geometric configuration of the beacons described in Section II has been simulated in Matlab® (see Fig. 1). The frequency response of the transducer has been considered, with bandwidth of 18 kHz around a central frequency of 40 kHz. In consequence, $J=5$ Kasami sequences with good cross-correlation properties among them and length $L=1023$ have been modulated with two ($N_{SM}=2$) symbols of a $f_c=40$ kHz carrier cycle. Therefore, the total duration of the five simultaneous emissions is of 51.15 ms.

49 Test positions (1-49) have been defined in a grid over the floor (see Fig. 9). For each one of the 49 positions we have measured four TDOAs at 39 different time instances. In Fig. 10 the mean error and the standard deviation in the x-axis and y-axis are shown only for odd test position. For comparison purposes, Fig. 11 shows the results for the same positions when the processing is carried out by a traditional U-LPS$_T$ receiver system, as the one indicated in Fig. 6. In both cases a SNR=0 dB has been considered. Fig. 12 depicts the Cumulative Distribution Function (CDF) considering all the evaluated positions, both for the proposed U-LPS$_N$ and a U-LPS$_T$. On average, the LPS$_N$ produces positioning accuracies around 5 cm, with standard deviations below 4 cm in most of the cases. Results with the LPS$_T$ are slightly better, with average accuracies approaching 4 cm and standard deviations below 3 cm. Positions located close to a specific beacon, such as position 31 or 25, can be more affected by the near-far effect. On the other hand, positions being far away from the beacons receive the emitted signals more attenuated and can be more affected by the noise, what means an increase of standard deviations (see results for positions 35 or 43).

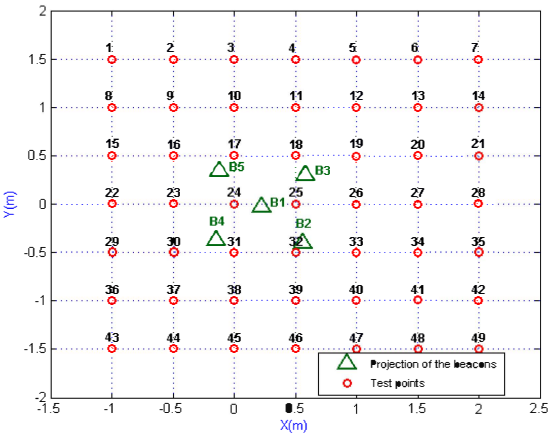

Fig. 9.- Test positions and beacon projections in the ground.

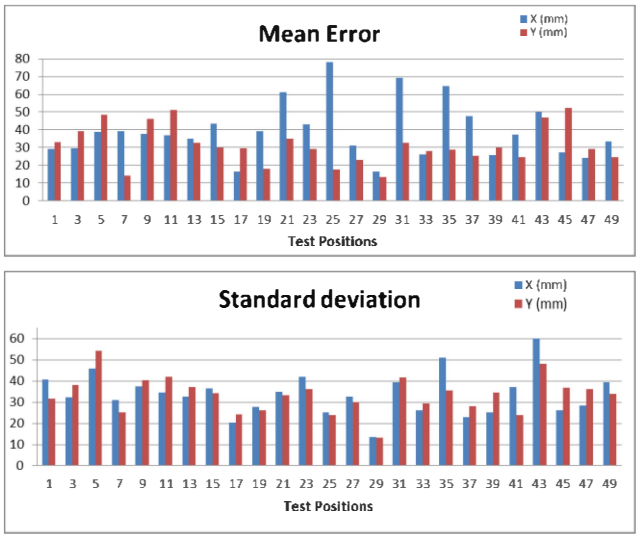

Fig. 10.- Simulated average and standard deviation of errors in mm, when using the LPS_N.

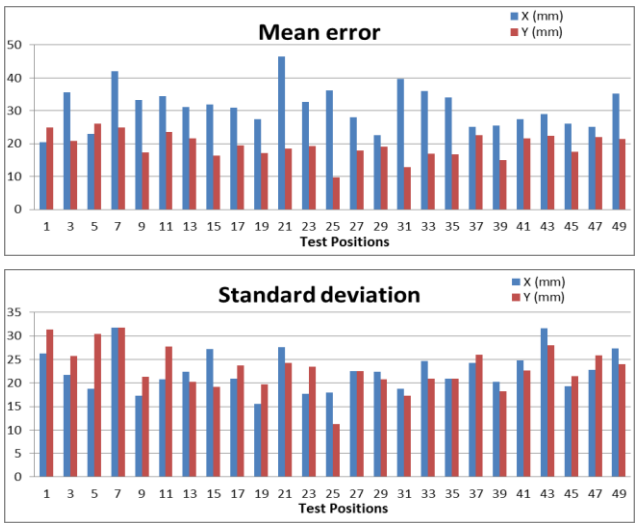

Fig. 11.- Simulated average and standard deviation of errors in mm, when using a U-LPS_T.

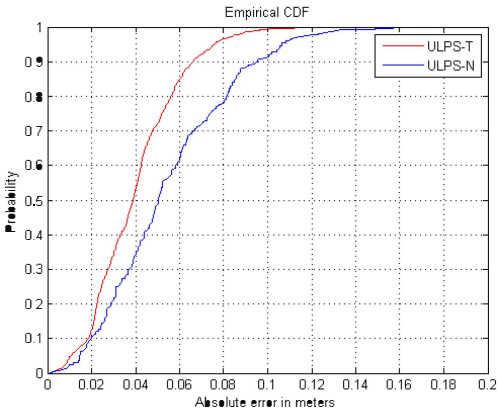

Fig. 12.- CDF for the 49 evaluated test positions, both for the U-LPS_N and U-LPS_T with simulated results.

B. RESULTS WITH REAL SIGNALS

Some real test has been carried out in order to verify the proposed detection module for smartphones. The same test points as the ones indicated in Fig. 9 have been considered, for each test point 39 measurements have been made. Fig. 13 is a photo of the experimental set-up for the test carried out. The receiver is a Brüel & Kjaer 4939 microphone [18]. It has a sensitivity of 4 mV/Pa in the frequency range that goes from 4 kHz to 100 kHz. It has been connected to an adjustable preamplifier, which output has been captured by an ultrasonic acquisition system of Avisoft (UltraSound Gate 116Hm [19]).

For comparison purposes, two processing alternatives have been carried out:

- U-LPS_T: the received signal has been sampled at 400 kHz and then the low level and high level tasks have been directly performed to obtain the receiver position.
- U-LPS_N: the received signal has been translated in frequency as described in Section III. Then, it has been sampled at 44 kHz and the low-level and high level tasks have been carried out.

Fig. 14 shows the results obtained for each test position with the U-LPS_N. For every test point, the ellipse represents the 95 % confidence level absolute position obtained. All position tests have been correctly identified, even those far away from the beacons or more affected by the multipath (such as positions 43 or 49 which are close to a wall). Fig. 15 depicts the CDF for the evaluated positions, both for the proposed U-LPS_N and a U-LPS_T. Note that the U-LPS_N offers absolute errors below 6 cm in 80% of the cases; whereas in the U-LPS_T errors in 80% of the cases are below 2.5 cm. Both the results of simulated and real data for the U-LPS_T and U-LPS_N offer a similar behavior, as can be seen in Figs. 12 and 15. Nevertheless, simulated results have been obtained with a lower SNR (0 dB in contrast to the 30 dB of the real-test); and with a very restrictive beacon transducer model, which offers worst results than the real one.

Fig. 13.- Environment used to perform the ranging test.

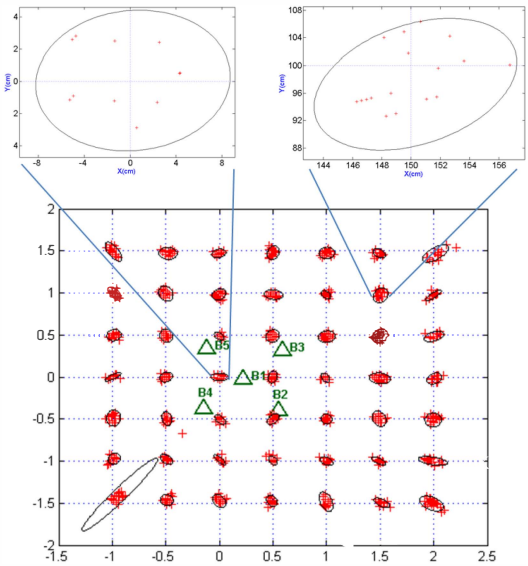

Fig. 14.- Position obtained with a 95% confidence level in the U-LPS$_N$.

Although the proposed U-LPS$_N$ does not reach the accuracies of the U-LPS$_T$, results are still very competitive if compared with LPS for smartphones based on RF (around 10 m in Skyhood commercial system [3]; 3 m with the hybrid fingerprinting technique presented in [1]; or 2 m in the strength-based method proposed in [2]). It also outperforms accuracies achieved in [8] which uses centralized U-LPS for

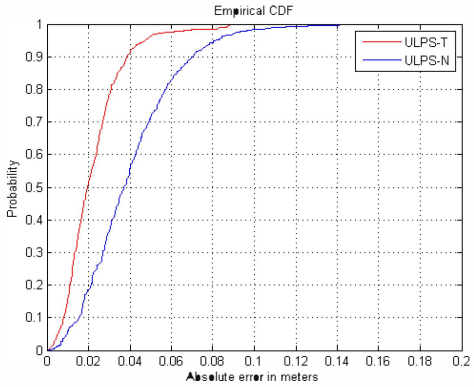

Fig. 15.- Empirical CDF for the 49 evaluated test positions, both for the U-LPS$_N$ and U-LPS$_T$.

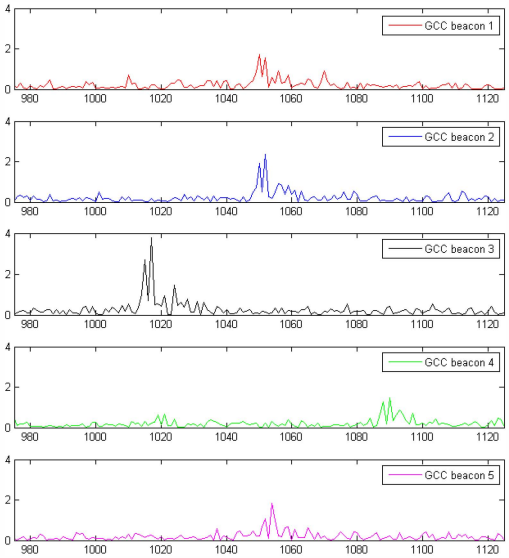

Fig. 16.- Absolute value of aperiodic GCC for the real ultrasonic signal captured in position 7 (x = 2 m; y=1,5 m).

indoor positioning of smartphones. Furthermore, in contrast to U-LPS$_T$, when smartphones or tablets are used as receivers the user can also benefit from all the possibilities that these platforms offer. As well as this, the proposed system can be used in extended areas if several U-LPS$_N$ are considered, each one covering a particular zone of the total area. Then, when the user is in a place where any U-LPS$_N$ is available, the position can be computed by using the smartphone odometer information as shown in [11].

Now we analyze thoroughly the test positions 7 (x = 2 m; y=1.5 m) and 24 (x=0 m; y=0 m). Fig. 16 shows the absolute value of the GCC associated to each beacon emission for the position 7, which is placed far away from the beacons, especially from beacon B4. As a result, the correlation peak

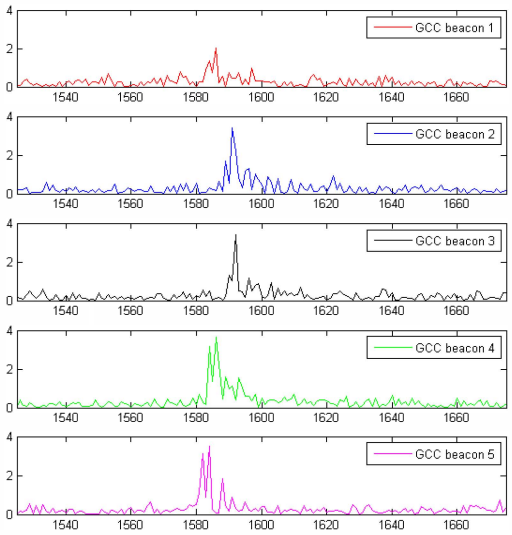

Fig. 17.-Absolute value of aperiodic GCC for the real ultrasonic signal captured in position 24 (x=0 m; y=0 m).

that indicates the arrival instant of the emission from that beacon is the one that appear more attenuated. Anyway, average and standard deviations for that position are $(\bar{x},\bar{y})$=(2.0114; 1.4667) mm and $(\sigma_x;\sigma_y)$=(0.0345; 0.0359) mm, respectively. Fig. 17 is the absolute value after the GCC for every beacon, in position 24. This position is more close to beacon B5 than to beacons B2 or B3. However since the beacons are placed next to the others (see Fig. 2 for the geometrical distribution of the beacons), the near-far effect is not relevant, and signals from the different beacons are received with similar signal-strength. Average and standard deviations for position 24 are $(\bar{x},\bar{y})$=($2.5\cdot10^{-3}$; $5.1945\cdot10^{-5}$) mm and $(\sigma_x;\sigma_y)$=(0.0355; 0.0168) mm respectively.

V. CONCLUSIONS

This paper has presented a low-cost CDMA based U-LPS for portable devices, such us smartphones or tablets. It is privacy oriented, and to achieve multi-emission the signals emitted from the beacons have been encoded with Kasami codes. In the reception, an external hardware device has been designed which translates the high-frequency signals coming from the beacons (which normally operate around 40 kHz), into the band available for current mobile phone microphones (below 22 kHz). The proposed hardware includes a standard ultrasonic microphone, an analog multiplier and a low-pass filter. The ultrasonic microphone acquires the signal coming from the U-LPS beacons, and multiplies it by a cosine so as to perform the frequency down translation. Then a low-pass filter removes the high frequency components. The output of the filter is connected to the smartphone or tablet by using the Jack input connector. After, the mobile device computes the generalized-cross correlation function (GCC) for obtaining the differences in times of arrival (TDOA) between the receptions of the signals coming from the different beacons. The pattern for the GCC is stored in memory of the mobile device and consists in the ideal modulated codes after being translated into low frequency. Once the TDOA are computed, the mobile device computes its position by hyperbolic trilateration.

The proposal has been tested either with simulated and real data. Furthermore, its performance has been compared with that obtained with the original U-LPS using an ultrasonic receiver with its ad-hoc hardware. The results show centimeter accuracy (below 6 cm in 80% of the cases) with real signals.

ACKNOWLEDGMENT

This work has been supported by the University of Alcalá and the Spanish Ministry of Economy and Competitiveness (LORIS project, ref. TIN2012-38080-C04-01, DISSECT-SOC project, ref. TEC2012-38058-C03-03) and the fellowship FPI/UAH program.

REFERENCES

[1] P. Mestre, C. Serodio, L. Coutinho, L. Reigoto, j. Matias, "Hybrid technique for fingerprinting using IEEE802.11 Wireless Networks," Proceedings of 2011 International Conference on Indoor Positioning and Indoor Navigation (IPIN), Guimaraes, Portugal, September, 2011.

[2] B. Ferris, D. Hähnel, D. Fox, "Gaussian Processes for Signal Strength-Based Location Estimation," Proceedings of Robotics Science and Systems, Philadelphia, PA, USA, pp. 16-19, August, 2006.

[3] C. Steger, "Massive Scalable Indoor Positioning: the Skyhook solution," available online: http://www.cwins.wpi.edu/workshop12/presentation/Technology_panel/chris_steger.pdf (accessed on 22 July 2013).

[4] M. Hazas and A. Hooper, "Broadband ultrasonic location system for improved indoor positioning," IEEE Trans. On Mobile Computing vol. 5, no. 8, pp. 536-547, May 2006.

[5] J. C. Prieto, A. R. Jiménez, J. Guevara, J. Ealo, F. Seco, J. Roa and A. Kotsou, "performance evaluation of 3D-LOCUS advanced acoustic LPS," IEEE Transactions on Instrumentation and Measurement, vol. 58, no. 8, pp. 2385-2395, August 2009.

[6] M. C. Pérez, R. Sanz, J. Ureña, A. Hernández, C. De Marziani, F. J. Álvarez, "Correlator implementation for Orthogonal CSS used in an Ultrasonic LPS," IEEE Sensors Journal, Vol. 12, No. 9, pp. 2807-2816, September 2012.

[7] J. Ureña, A. Hernández, A. Jiménez, J. M. Villadangos, M. Mazo, J. C. García, J. J. García, F. J. Álvarez, C. De Marziani, M. C. Pérez, J. A. Jiménez, A. R. Jiménez, F. Seco, "Advanced sensorial system for an acoustic LPS," Microprocessors and Microsystems, February 2007.

[8] V. Filonenko, C. Cullen, J. Carswell, "Indoor Positioning for Smartphones using asynchronous ultrasound trilateration," ISPRS International Journal of Geo-Information, June 2013.

[9] M. Hazas, A. Ward, "A high performance privacy-oriented location system," Proceedings of the First IEEE International Conference on Pervasive Computing and Communications (PerCom'03), Fort Worth , Texas, USA, March 2003.

[10] D. Ruíz, J. Ureña, J. C. García, C. Pérez, J. M. Villadangos, E. García, "Efficient trilateration algorithm using time differences of arrival," Sensors and Actuators A: Physical, Vol. 193, pp. 220-232, 2013.

[11] D. Ruíz, E. García, J. Ureña, D. de Diego, D. Gualda, J. C. García, "Extensive Ultrasonic Local Positioning System for navigating with mobile robots," Workshop on Positioning Navigation and Communications (WPNC), pp. 1-6, Dresden (Germany), March 2013.

[12] T. Kasami, "Weight distribution formula for some class of cyclic codes," Technical reportR-285, Coordinated Science Lab. University of Illinois, April 1968.

[13] Prowave 328ST160, Product specification, available online: http://www.prowave.com.tw/english/products/ut/open-type/328s160.htm, (accessed on 22 July 2013).

[14] Tabor Electronics Arbitrary Waveform Generator WW5062, Product specification, Available online: http://www.taborelec.com/products_home.asp?prod=arbitrary_waveform_function_generator&model=WW5062&over=products&prod3=dual_channel_arbitrary_waveform_generators, (accessed on 22 July 2013).

[15] C. H. Knapp, G. C. Carter, "The Generalized Correlation Method for Estimation of Time Delay," IEEE Transactions of Acoustics, Speech and Signal Processing, Vol. ASSP-24, No. 4, August 1976.

[16] J. M. Villadangos, J. Ureña, J. J. García, M. Mazo, A. Hernández, A. Jiménez, D. Ruíz, C. De Marziani, "Measuring Time-of-Flight in an Ultrasonic LPS System Using Generalized Cross-Correlation," Sensors 2011, vol. 11, pp. 10326-10342, 2011.

[17] A. Hernández, J. Ureña, J. J. García, M. Mazo, D. Hernanz, J.Sérot, "Ultrasonic ranging sensor using simultaneous emissions from different transducers," IEEE Transactions on Ultrasonics, Ferroelectrics , and Frequency Control, Vol. 51, no. 12, pp. 1660- 1670, December 2012.

[18] Brüel&Kjaer microphone, product specification, available online: http://bksv.es, (accessed on 22 July 2013).

[19] Avisoft Bioacoustics, product specification, available online: http://www.avisoft.com, (accessed on 22 July 2013).